

## On the Phase Relations between the Western North Pacific, Indian, and Australian Monsoons\*

DEJUN GU

*Guangzhou Institute of Tropical and Marine Meteorology, and Key Open Laboratory for Tropical Monsoon, China Meteorological Administration, Guangzhou, China*

TIM LI

*International Pacific Research Center, and Department of Meteorology, University of Hawaii at Manoa, Honolulu, Hawaii*

ZHONGPING JI

*Guangzhou Central Meteorological Observatory, Guangzhou, China*

BIN ZHENG

*Guangzhou Institute of Tropical and Marine Meteorology, and Key Open Laboratory for Tropical Monsoon, China Meteorological Administration, Guangzhou, China*

(Manuscript received 31 July 2008, in final form 4 March 2010)

### ABSTRACT

The phase relationships of the western North Pacific (WNP) summer monsoon (WNPM) with the Australian monsoon (AM) and Indian monsoon (IM) are investigated using observational rainfall, SST, and NCEP reanalysis data for the period of 1979–2005. It is found that a strong WNPM often follows a strong AM but leads a weak AM, and a significant simultaneous negative correlation appears between WNPM and IM. The in-phase relationship from AM to the succeeding WNPM occurs often during the El Niño decaying phase when the warm eastern Pacific SST anomaly (SSTA) weakens AM through anomalous Walker circulation and the persistence of an anomalous WNP anticyclone from the boreal winter to summer leads to a weak WNPM. The out-of-phase relation from WNPM to the succeeding AM occurs either during the El Niño early onset year when the warm SSTA in June–August (JJA) is strong enough to force a low-level cyclonic flow anomaly in WNP and in December–February (DJF) the same warm SSTA forces a weak AM, or during the El Niño decaying phase when the persistence of the WNP anomalous anticyclone causes a weak WNPM and the transition of a warm to a cold episode causes a strong AM in DJF. The simultaneous negative correlation between WNPM and IM often appears either during the El Niño early onset years when the warm eastern Pacific SSTA induces the cyclonic wind shear that strengthens WNPM but suppresses convection over India, or during the El Niño decaying summer when a weak WNPM results from the persistence of the local anomalous anticyclone and a strong IM results from the El Niño-to-La Niña transition or a basin-wide Indian Ocean warming.

---

### 1. Introduction

The tropical monsoon system in the Indo-Pacific warm pool region consists of three submonsoon components: the Indian monsoon (IM), the western North Pacific monsoon (WNPM), and the Australian monsoon (AM). Observations show that there is an in-phase relation between IM and the subsequent AM (Meehl 1987; Chang and Li 2000; Hung et al. 2004; Zhang and Li 2008). A

---

\* School of Ocean and Earth Science and Technology Contribution Number 7906 and International Pacific Research Center Contribution Number 682.

*Corresponding author address:* Dejun Gu, Guangzhou Institute of Tropical and Marine Meteorology, and Key Open Laboratory for Tropical Monsoon, China Meteorological Administration, Guangzhou 510080, China.  
E-mail: djg@grmc.gov.cn

strong (weak) AM often follows a strong (weak) IM a half year later. By analyzing observed precipitation data for the period of 1901–71, Gregory (1991) noted that the AM rainfall amount has a close relationship with the preceding IM rainfall, but it has no significant correlation with the succeeding IM rainfall. Thus, there is an asymmetric relationship between the two submonsoon systems, and a forecast barrier appears in boreal spring prior to the onset of the Indian summer monsoon. Matsumoto (1992) showed that the advances and retreats of the Indian and Australian monsoons are closely related.

Four possible mechanisms have been proposed to explain the in-phase relationship between the IM and AM rainfall anomalies: 1) southeastward propagation of seasonal convective maximum (Meehl 1987), 2) IM convective heating–western Pacific SST teleconnection (Chang and Li 2000), 3) ENSO remote forcing mechanism (Hung et al. 2004), and 4) Indian Ocean SSTA propagation (Zhang and Li 2008). Meehl (1987) noted that convection anomalies associated with tropospheric biennial oscillation (TBO) move southeastward from India during boreal summer to northern Australia during boreal winter as the annual cycle of the seasonal convective maximum also proceeds southeastward from the Northern Hemisphere (NH) summer to the Southern Hemisphere (SH) summer. Chang and Li (2000) suggested that a strong Indian summer monsoon may intensify a planetary-scale east–west circulation leading to anomalous easterlies over the western Pacific and Maritime Continent, which reduce surface evaporation and leads to a warm SST anomaly (SSTA). The local warm SSTA persisting from northern fall to the subsequent winter leads to a stronger AM. Hung et al. (2004) argued that the in-phase relation is simply the response of IM and AM to the remote El Niño forcing through anomalous Walker circulation as the eastern Pacific SSTA persists from its developing summer to its mature winter. The reversed relationship from AM to the subsequent IM is unclear because the effect of the eastern Pacific SSTA diminishes during the ENSO decaying summer. Zhang and Li (2008) noted that 60% of the IM–AM in-phase cases are related to ENSO events, while the others are not. A further analysis reveals that a major feature in the non-ENSO composite is the eastward propagation of SSTA in the tropical IO from northern summer to winter that connects the Indian and Australian monsoons. Fasullo (2004) suggested the role of ENSO in the biennial variability of the Indian monsoon. Wu and Kirtman (2007a,b) proposed that the biennial transition of the IM may result from air–sea interactions in the northern Indian Ocean and that air–sea coupling in the Indian Ocean plays a role in maintaining the negative AM–ENSO relationship. The monsoon–ENSO relation has experienced a marked

interdecadal variation (Kumar et al. 1999; Krishnamurthy and Goswami 2000; Chang et al. 2001).

While many previous studies focused on the IM and AM phase relation, little work has been done on the phase relationships of WNPM with IM and AM. The precipitation anomaly in the WNPM region exhibits a remarkable quasi-biennial variability, which may result from either a remote ENSO forcing or warm pool ocean–atmosphere interactions (Li et al. 2006). The objective of this research is to reveal the WNPM phase relations with other submonsoon systems and to understand the possible causes of the phase relationships. Specific questions to be addressed include: What are lagged phase relations between WNPM and AM, and what are physical processes that connect the two submonsoon systems if significant lagged correlations do exist between them? What is the simultaneous relationship between WNPM and IM and why? Understanding these questions will no doubt help improve the monsoon seasonal prediction.

The rest of this paper is organized as follows. In section 2, the datasets and methods used in this study are described. In section 3, we examine the observed phase relationships among the three submonsoon systems by introducing the monsoon intensity indices for each of the submonsoon systems. In section 4, we examine the evolution characteristics of precipitation and circulation patterns. In section 5, we provide a physical interpretation for each type of in-phase and out-of-phase relationships. Finally, a summary is given in section 6.

## 2. Data and methods

The primary data used in this study are the National Centers for Environmental Prediction (NCEP) Department of Energy (DOE) Atmospheric Model Intercomparison Project (AMIP-II) reanalysis (R-2) products from 1979 to 2005 (Kanamitsu et al. 2002). These monthly data have a horizontal resolution of 2.5° latitude by 2.5° longitude and 12 pressure levels vertically. The monthly mean rainfall fields are from the Climate Prediction Center (CPC) Merged Analysis of Precipitation data (CMAP; Xie and Arkin 1997) and the monthly mean SST fields are from the National Oceanic and Atmospheric Administration (NOAA) Extended Reconstructed SST V2 (see online at <ftp://ftp.ncdc.noaa.gov/pub/data/ersst-v2/>; Smith and Reynolds 2004) for the period of 1979–2005. To validate the data above, additional datasets such as Global Precipitation Climatology Project (GPCP) monthly precipitation data (see online at <http://precip.gsfc.nasa.gov/>; Adler et al. 2003), the Japanese 25-yr Reanalysis Project (JRA-25) data (Onogi et al. 2007), the precipitation reconstruction dataset (PREC; see online at [ftp://ftp.cpc.ncep.noaa.gov/precip/50yr/land\\_ocean/format\\_bin/](ftp://ftp.cpc.ncep.noaa.gov/precip/50yr/land_ocean/format_bin/);

Chen et al. 2004), and the NCEP–National Center for Atmospheric Research (NCAR) reanalysis products (Kalnay et al. 1996) are used.

The Niño-3.4 index is obtained online (see <http://www.cdc.noaa.gov/ClimateIndices/List/>). The El Niño and La Niña episodes are defined based on the CPC criterion when the threshold of  $\pm 0.5^{\circ}\text{C}$  is met for a minimum of five consecutive overlapping seasons (see online at [http://www.cpc.noaa.gov/products/analysis\\_monitoring/ensostuff/ensoyears.shtml](http://www.cpc.noaa.gov/products/analysis_monitoring/ensostuff/ensoyears.shtml)). The early onset of El Niño–La Niña events refers to the amplitude of the seasonal mean Niño-3.4 SSTA exceeding  $0.5^{\circ}\text{C}$  prior to June–August (JJA). The La Niña persistence event refers to the cold episode that persists from the previous mature winter to the subsequent winter.

The analysis methods used in this study include correlation, regression, and composite analyses. A Student's *t* test is used to measure the statistical significance of correlations. The significance level for the composite fields is assessed using the Monte Carlo techniques based on Livezey and Chen (1983) and Wolter et al. (1999). Different from many previous studies that made composites based on El Niño and La Niña conditions, here we compose based on the monsoon intensity first, and then for each monsoon phase relation we further group the events based on various ENSO phases. The definitions of the monsoon intensity and the ENSO phase are defined in the next section.

### 3. Observed phase relations among the three submonsoon systems

#### a. Definition of the WNPM, IM, and AM intensity

Conventionally, the monsoon intensity is defined by the average of rainfall or circulation (including wind or vorticity) over a particular region where both the mean and variability are great. Figure 1 shows the mean and standard deviation of precipitation and vorticity fields in boreal winter and summer, respectively, based on NCEP R-2 and the CMAP dataset. During boreal winter, maximum mean precipitation occurs near and south of the equatorial oceans and over the Maritime Continent and northern Australia. The large standard deviation centers appear over the South China Sea (SCS), east of Philippines, WNP, and northeast Australia. During boreal summer, maximum seasonal mean rainfall centers move to the Northern Hemisphere, and are located at the southwest of India, Bay of Bengal (BOB), SCS, and tropical WNP. The regions of large standard deviation are in generally collocated with the maximum mean precipitation regions. The characteristics of the relative vorticity field at 850 hPa are similar to those in the rainfall

field, with large mean and standard deviation of relative vorticity over the northern Australia during boreal winter and over India/BOB, SCS, and WNP during boreal summer. Thus, the regions of the Indian monsoon, WNP monsoon, and Australia monsoon are characterized by maximum mean and standard deviation in both the rainfall and vorticity fields in their local summer.

In the following we define the monsoon intensity index for each submonsoon region according to the distribution characteristics of the mean and standard deviation in precipitation and 850-hPa relative vorticity fields. The intensity of WNPM is defined as the relative vorticity value averaged over the region of  $10^{\circ}\text{--}20^{\circ}\text{N}$ ,  $110^{\circ}\text{--}140^{\circ}\text{E}$  during June–August, whereas the intensity of IM is defined as the mean rainfall averaged over  $5^{\circ}\text{--}20^{\circ}\text{N}$ ,  $70^{\circ}\text{--}90^{\circ}\text{E}$  during June–August and the intensity of AM is defined as the mean rainfall averaged over  $20^{\circ}\text{--}5^{\circ}\text{S}$ ,  $130^{\circ}\text{--}160^{\circ}\text{E}$  during December–February (DJF). Figure 2 illustrates the time series of the three monsoon intensity indices.

The circulation index in WNP well represents the WNPM rainfall variability. In fact, the correlation coefficient between the WNPM circulation and rainfall indices is 0.64, exceeding the 99% significant level. Figure 3 shows the simultaneous precipitation correlation patterns and 850-hPa wind regression patterns in association with the WNPM, AM, and IM indices, respectively. They are all significantly positively correlated with local precipitation and low-level cyclonic vorticity anomalies. Besides representing the local precipitation and low-level cyclonic flow, the WNPM circulation index also has a significant negative correlation with rainfall over northern Indian Ocean.

#### b. Phase relations among WNPM, IM, and AM

Table 1 shows the correlations among the time series of the WNPM, AM, and IM intensity indices from 1979 to 2005. The correlation coefficient between WNPM and the preceding AM is 0.37, passing the 90% significance level. This implies that a strong (weak) AM might be associated with a succeeding strong (weak) WNPM. This in-phase relation appears in 19 out of the total 27 years. Table 2 lists specific years for the in-phase relationship. For easy comparison, in the table we also list the corresponding winter (DJF) Niño-3.4 index. In the following composite analysis, only cases in which both the monsoon intensity indices exceed 0.4 standard deviation are considered and named as strong events. (A sensitivity test with a 0.5 standard deviation threshold shows similar composite results.) Note that the eastern Pacific SSTA is all positive (negative) for the negative (positive) strong in-phase events, implying that ENSO is a major controlling factor for the AM–WNPM in-phase relationship.

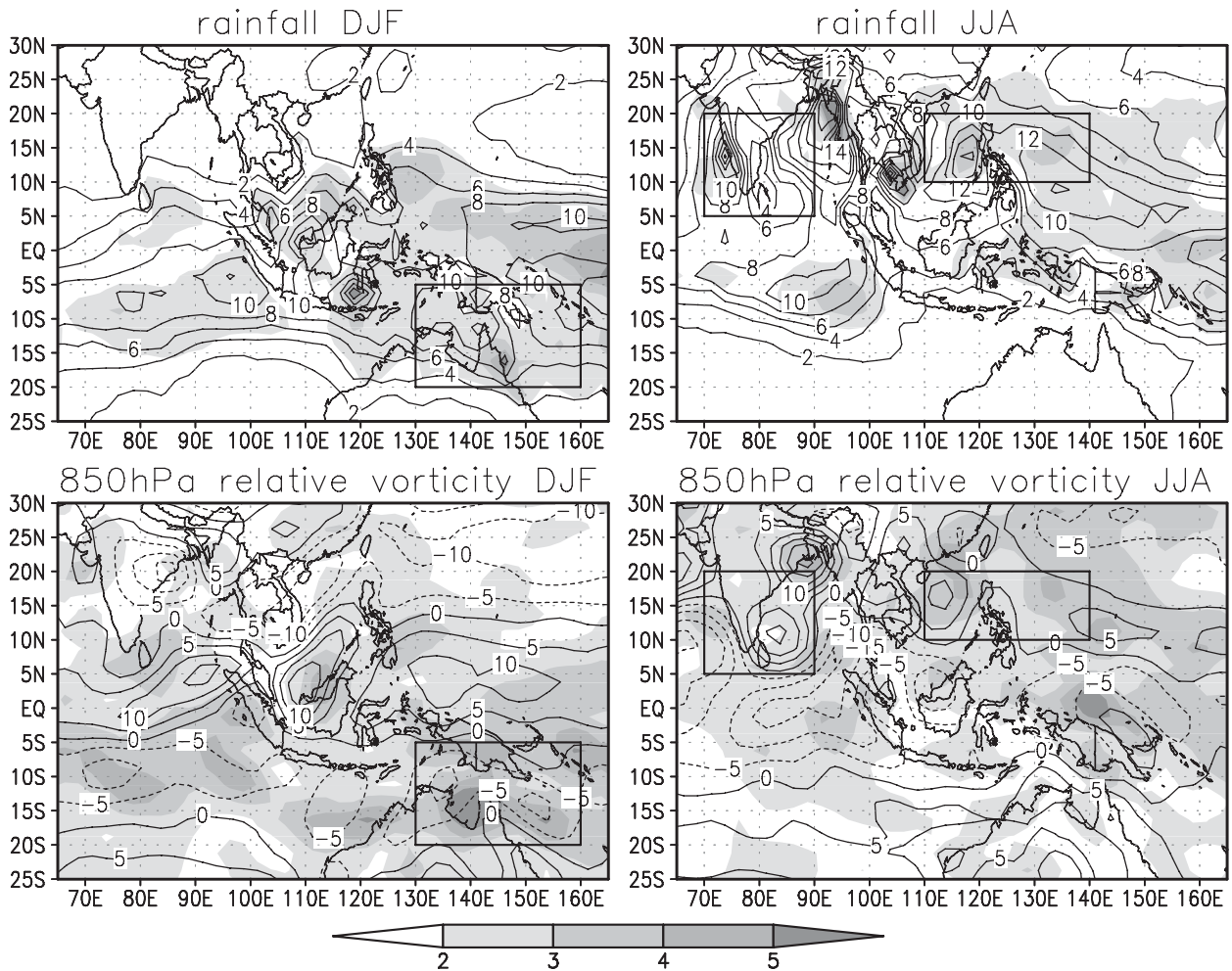


FIG. 1. Mean (contour) and standard deviation (shaded) of (top) rainfall (unit:  $\text{mm day}^{-1}$ ) and (bottom) relative vorticity at 850 hPa ( $10^{-6} \text{ s}^{-1}$ ) during (left) boreal winter and (right) summer, based on NCEP R-2 and CMAP dataset. The black boxes denote the three submonsoon domains, respectively. For the mean precipitation, only contour lines that are  $\geq 6 \text{ mm day}^{-1}$  are plotted. For the mean vorticity, only contour lines with positive (negative) values in JJA (DJF) are plotted.

The correlation coefficient between WNPM and the succeeding AM is  $-0.41$ , exceeding the 95% significance level. This points out an out-of-phase relation between the two submonsoon systems, that is, a strong (weak) WNPM often leads a weak (strong) AM. A further examination shows that about  $\frac{2}{3}$  of all events reflect the out-of-phase relationship. Table 3 shows the cases for the out-of-phase relationship between WNPM and the succeeding AM, along with the corresponding JJA Niño-3.4 index. Again, only those cases in which the standard deviation of both the monsoon intensity indices exceeds 0.4 are selected for the composite analysis.

The most significant correlation appears in the simultaneous correlation between WNPM and IM, which is  $-0.64$ , passing the 99% significance level. This simultaneous out-of-phase relation appears in 17 summers during 1979–2005. Table 4 lists all out-of-phase monsoon

(between WNPM and IM) events and the corresponding summer Niño-3.4 index.

As seen from Table 1, compared with the correlations between the WNPM and AM–IM, the correlation coefficients between IM and AM are relatively weak. The sensitivity of the relationships to different datasets will be discussed in section 5. In this study we focus on the phase relationships of WNPM with the preceding and succeeding AM and the simultaneous IM.

To illustrate the precipitation and circulation patterns associated with the in-phase and out-of-phase WNPM–AM relationships, we show the lagged correlation and regression patterns 6 months after WNPM and 6 months after AM in Fig. 4. Note that the WNPM is significantly negatively correlated with the precipitation a half year later over the Maritime Continent. Six months after a strong AM, positive rainfall and cyclonic flow anomalies

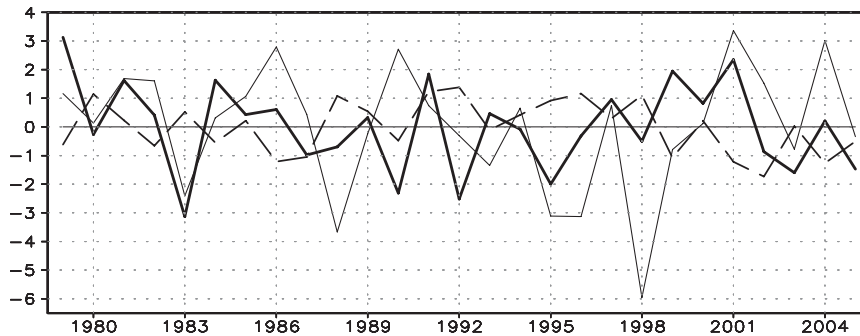


FIG. 2. Time evolution of Australian (thick solid line), Indian (dashed line), and western North Pacific (thin solid line) ( $\times 10^{-6} \text{ s}^{-1}$ ) summer monsoon intensity indices for 1979–2005 ( $\text{mm day}^{-1}$ ).

appear over WNP, confirming the in-phase relation between AM and the subsequent WNPM.

The significant simultaneous negative correlation between WNPM and IM can be inferred from the top and bottom panels of Fig. 3. When the WNPM is strengthened, India is controlled by an anomalous ridge and deficient rainfall anomalies that extend from the Maritime Continent northwestward. When the IM is strengthened, an anomalous anticyclone and negative rainfall anomalies appear over the WNP–SCS region.

#### 4. Circulation patterns associated with the in-phase and out-of-phase monsoon relations

The observational data analysis above points out a 6-month lead–lag relation between WNPM and AM. As the anomalous rainfall and wind signals in the atmosphere alone cannot hold such a long memory, the phase relationships between WNPM and the AM six months later requires a physical explanation.

As described in the introduction section, both the remote ENSO impact and local air–sea interactions may play a role in connecting the submonsoon systems. To examine the possible ENSO effect, we first calculate the lagged correlation coefficient between the seasonal mean Niño-3.4 index and the WNPM, AM, and IM indices (Fig. 5). Note that the simultaneous correlation coefficient between DJF Niño-3.4 index and the AM index is  $-0.63$ , exceeding the 99% significance level. Within the 27-yr period (1979–2005), there are 22 boreal winters during which the AM rainfall anomaly is opposite to the Niño-3.4 SSTA. This demonstrates that the ENSO has a strong impact on the Australian summer monsoon. The lagged correlation between DJF Niño-3.4 index and WNPM in the subsequent summer is  $-0.45$ , exceeding the 98% significance level. The simultaneous correlation of WNPM with the JJA Niño-3.4 index is also significant. On the other hand, the simultaneous

correlation of IM with the JJA Niño-3.4 index is  $-0.31$ , hardly passing the 90% significance level.

In the following we first describe the observed circulation and SST changes associated with the monsoon in-phase and out-of-phase relationships. Then in the subsequent section we will further discuss possible mechanisms responsible for the three intermonsoon phase relationships, all of which involve WNPM.

##### a. In-phase relation between AM and the succeeding WNPM

To illustrate specific processes that maintain the in-phase relation between AM and the succeeding WNPM, we conduct a composite analysis. Because the strong and weak in-phase composites are approximately mirror images, we show only the difference maps. Figure 6 shows the evolution from boreal winter to the subsequent summer of difference fields of SST, 850-hPa wind, and precipitation between strong and weak monsoon in-phase events. Please note that the AM–WNPM in-phase relation is clearly associated with the El Niño decaying phase.

During the El Niño mature winter, the ascending branch of the anomalous Walker cell is located over the equatorial central Pacific, while a descending branch appears over the Maritime Continent and northern Australia. Anomalous easterlies and anticyclonic circulation control the northwest of Australia, which reduce moisture transport into the AM region. As a result, the Australian summer monsoon is weakened. Meanwhile, an anomalous anticyclone appears in WNP. This anomalous anticyclone is maintained from boreal winter to summer. Wang et al. (2003) suggested that the maintenance of the anticyclone anomaly is primarily through a positive feedback between the anticyclone and underlying cold SSTA in the presence of the mean northeasterly from boreal winter to late spring. The amplitude of the composite cold SSTA in WNP exceeds  $-0.6^{\circ}\text{C}$  in March–May

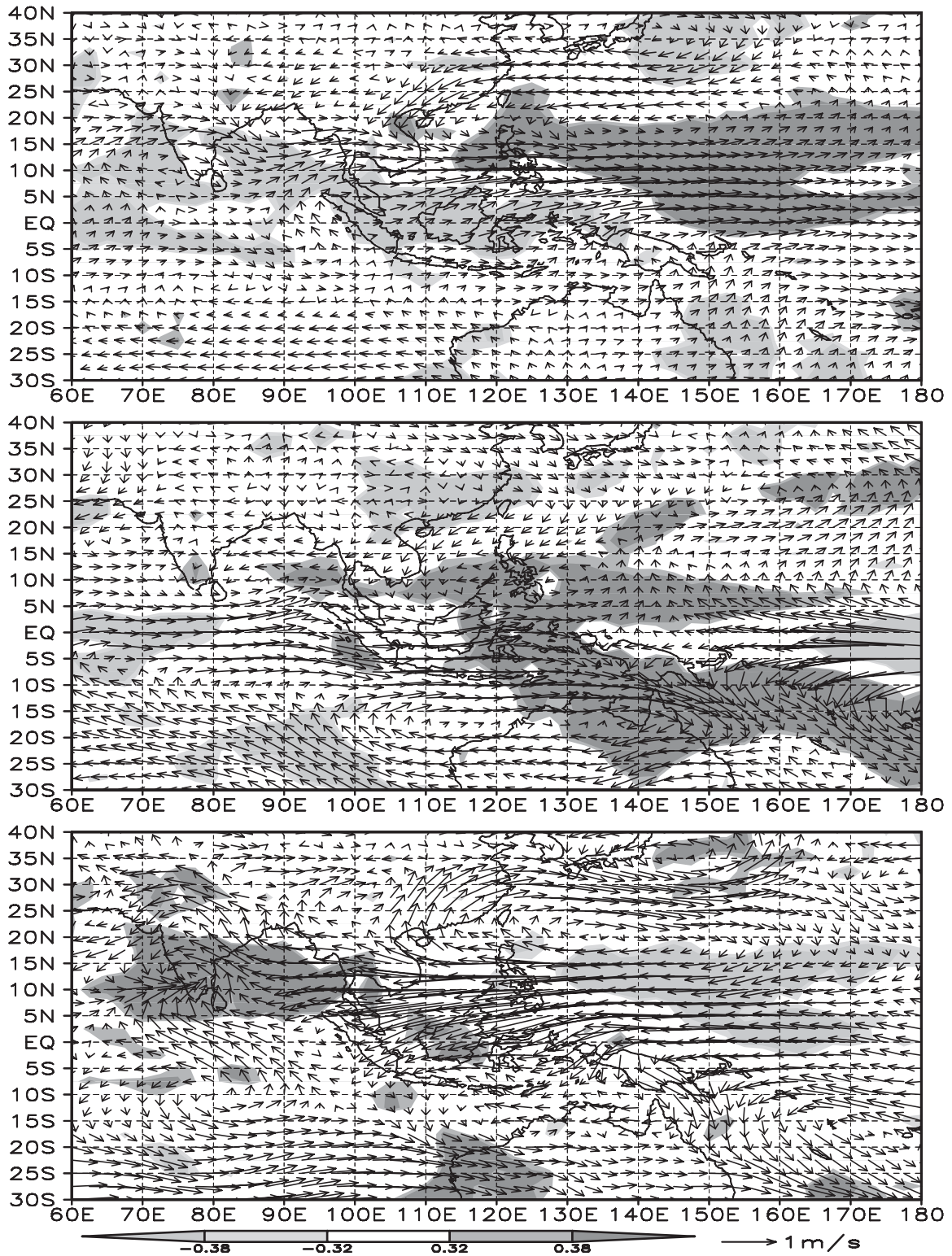


FIG. 3. Precipitation correlation patterns and 850-hPa wind regression patterns in association with the (top) WNP, (middle) Australian, and (bottom) Indian summer monsoon intensity indices. The areas exceeding the 90% and 95% significant level are shaded.

TABLE 1. Lagged correlation coefficients among WNP, IM, and AM for 1979–2005 using NCEP–DOE and CMAP. The 90% (95%) significance level corresponds to a correlation coefficient of 0.32 (0.38). The boldface indicates a correlation exceeding the 90% significance level. The number of events indicates the number of years during which the relationship between two monsoons is consistent with the correlation coefficient.

From To	India JJA(0) Australia DJF(1)	Australia DJF(0) India JJA(0)	SCS–WNP JJA(0) Australia DJF(1)	Australia DJF(0) SCS–WNP JJA(0)	SCS–WNP JJA(0) India JJA(0)
Correlation coef	0.29	–0.28	<b>–0.41</b>	<b>0.37</b>	<b>–0.64</b>
No. of events	17	17	<b>17</b>	<b>19</b>	<b>17</b>

(MAM). This large local cold SSTA prior to the monsoon onset may have a great impact on the subsequent WNP (Wu et al. 2010).

The composite analysis above suggests that the remote El Niño forcing and the maintenance of the WNP anticyclone from the El Niño mature winter to the subsequent summer hold a key for connecting the preceding AM to the succeeding WNP.

#### b. Out-of-phase relation between WNP and the succeeding AM

Based on the circulation and SST evolution features, the out-of-phase WNP–AM cases may be divided into two groups. Group 1 consists of cases of El Niño early onset (such as in 1982, 1986, 2002, and 2004) and La Niña persistence (1996). Figure 7 illustrates the composite (El Niño minus La Niña) precipitation, SST, and 850-hPa wind anomaly fields from boreal summer to the following winter for this scenario. Note that the amplitude of the composite SSTA difference in the eastern Pacific is quite large, exceeding 1.0°C in JJA. This is consistent with the enhanced convection in the composite map in the central equatorial Pacific. The atmospheric response to the equatorial heating causes low-level cyclonic shear anomalies over WNP (Gill 1980), which may further strengthen WNP through the boundary layer convergence.

As the equatorial Pacific SSTA matures toward the boreal winter, it weakens the Australian summer monsoon through the anomalous Walker circulation. Thus, it is the same sign of the remote eastern Pacific SSTA forcing that determines the out-of-phase monsoon transition from a strong (weak) WNP in boreal summer to a weak (strong) AM in boreal winter.

Group 2 consists of cases of El Niño decaying–La Niña developing (1983 and 1998) and La Niña decaying–El Niño Modoki (e.g., Ashok et al. 2007) developing (2001). Figure 8 illustrates the composite rainfall, SST, and 850-hPa wind evolution patterns in this scenario. As the WNP intensity is greatly affected by El Niño–La Niña in the preceding winter (Wu et al. 2010), we plot the evolution from the ENSO mature winter to the succeeding winter. During the El Niño (La Niña) peak winter, an anomalous low-level anticyclone (cyclone) develops

over WNP. This anomalous anticyclone (cyclone) is maintained from DJF to JJA, leading to a weak (strong) WNP.

During the ENSO decaying summer, the SST anomalies in the eastern equatorial Pacific diminish. Thus, this group differs from the previous one in that the strength of WNP is not determined by the simultaneous SSTA but controlled by the SSTA in the preceding winter. The decay of a strong El Niño is often accompanied with the onset of La Niña. As the cold SSTA develops in the equatorial Pacific toward boreal winter, an anomalous Walker cell leads to abnormal ascending motion over the Maritime Continent and northern Australia, leading to a strong Australian summer monsoon.

Therefore, the connection of the WNP and AM phases in the second scenario is attributed to the persistence of the WNP anomalous anticyclone (cyclone) and the phase transition of the eastern Pacific SSTA from a warm (cold) to a cold (warm) episode.

#### c. Simultaneous negative correlation between WNP and IM

The examination of the circulation and SST patterns associated with the WNP–IM negative correlation events reveals that the causes of the negative simultaneous correlation may be categorized into the two groups. The

TABLE 2. Cases of the all in-phase relation between AM and the succeeding WNP. Boldface indicates that the normalized values of both the monsoon intensity indices exceed 0.4. The right column lists the corresponding Niño-3.4 index in DJF (simultaneous with the AM season).

Positive AM, Niño-3.4 index, and positive WNP	Negative AM Niño-3.4 index and negative WNP
<b>1979 (–0.1)</b>	<b>1983 (2.3)</b>
<b>1981 (–0.3)</b>	<b>1988 (0.8)</b>
1982 (0)	1992 (1.8)
1984 (–0.5)	<b>1995 (1.2)</b>
1985 (–1.0)	1996 (–0.8)
<b>1986 (–0.4)</b>	1998 (2.4)
1991 (0.5)	2003 (1.1)
1997 (–0.4)	2005 (0.6)
2000 (–1.6)	
<b>2001 (–0.7)</b>	
2004 (0.4)	

TABLE 3. Cases of the out-of-phase relation between WNPM and the succeeding AM. Boldface indicates that the normalized values of both the monsoon intensity indices exceed 0.4. The right column lists the corresponding Niño-3.4 index in JJA (simultaneous with the WNPM season).

Positive WNPM, Niño-3.4 index, and negative AM	Negative WNPM, Niño-3.4 index, and positive AM
1979 (0.0)	<b>1983 (0.2)</b>
<b>1982 (0.8)</b>	1988 (−1.2)
<b>1986 (0.2)</b>	1992 (0.4)
1987 (1.5)	<b>1996 (−0.1)</b>
1991 (0.9)	<b>1998 (−0.8)</b>
1994 (0.6)	1999 (−0.9)
1997 (1.7)	2003 (0.3)
<b>2001 (0.2)</b>	
<b>2002 (0.9)</b>	
<b>2004 (0.7)</b>	

first group consists of either the El Niño early onset (1982, 1990, 2002, and 2004) or La Niña persistence (1996) cases. Figure 9 shows the composite (El Niño events of 1982, 1990, 2002, and 2004 minus the 1996 La Niña event) SST, precipitation, and 850-hPa wind fields for this scenario. Because of the El Niño earlier onset or La Niña persistence, the eastern Pacific SSTA in JJA has attained a certain magnitude. As seen from Fig. 9, the maximum composite SSTA difference in the equatorial central-eastern Pacific exceeds 0.6°C. This SSTA, through the equatorial anomalous heating, may induce low-level cyclonic shear anomalies in WNP and subsidence anomalies over the Maritime Continent. The former strengthens WNPM through boundary layer moisture convergences, while the latter suppresses IM through the Rossby wave response to the suppressed convection over the Maritime Continent (Wang et al. 2003). As seen from Fig. 9, the maximum positive rainfall anomaly is located around 150°E–180°, while the maximum negative rainfall anomaly appears over the Maritime Continent and tilts north-westward toward the India subcontinent.

The composite maps above imply that the major factor that causes the out-of-phase WNPM–IM relation is the remote eastern Pacific SSTA forcing in JJA. A key ingredient to connect the remote SSTA forcing to the simultaneous WNP and Indian summer monsoons is through twin atmospheric Rossby wave responses to the positive and negative heating anomalies in the equatorial central Pacific and the Maritime Continent, respectively. It is noted that the SSTA amplitude and pattern in the aforementioned cases are remarkably different. While El Niño in 1982 is a typical strong episode, El Niños in 1990, 2002, and 2004 are characterized by a modest warming in the central Pacific. The central Pacific warming episodes are named as El Niño Modoki (Ashok et al. 2007) or the warm pool El Niño. The cold episode in

TABLE 4. Cases of the out-of-phase relation between WNPM and IM. Boldface indicates that the normalized values of both the monsoon intensity indices exceed 0.4. The right column lists the corresponding Niño-3.4 index in JJA (simultaneous with the monsoon season).

Positive WNPM, Niño-3.4 index, and negative IM	Negative WNPM, Niño-3.4 index, and positive IM
<b>1979 (0.0)</b>	<b>1983 (0.2)</b>
<b>1982 (0.8)</b>	<b>1988 (−1.2)</b>
1984 (−0.3)	1989 (−0.3)
<b>1986 (0.2)</b>	1992 (0.4)
1987 (1.5)	<b>1995 (0.0)</b>
<b>1990 (0.3)</b>	<b>1996 (−0.1)</b>
<b>2001 (0.2)</b>	<b>1998 (−0.8)</b>
<b>2002 (0.9)</b>	2003 (0.3)
<b>2004 (0.7)</b>	

1996 persists throughout the year. Although the cold SSTA center ( $\sim -0.9^\circ\text{C}$ ) appeared in the far eastern equatorial Pacific in JJA, the anomalous equatorial easterly and off-equatorial anticyclonic shear associated with the cold SSTA forcing may reach far to the Indo-western Pacific warm pool.

The second group consists of the El Niño decaying–La Niña developing (such as in 1983, 1988, 1995, and 1998) and the La Niña decaying–El Niño developing (1986) cases. Figure 10 illustrates the composite (El Niño decaying minus La Niña decaying) events from the preceding ENSO mature winter to the following summer. During the El Niño mature winter, an anomalous low-level anticyclone develops over WNP. It is maintained from DJF to JJA and leads to a weak WNP summer monsoon. For the La Niña early onset cases (1988, 1995, and 1998), the anticyclone can be further enhanced by the cold SSTA in the eastern Pacific in JJA, through a direct Gill-type response. The cold SSTA may enhance the convection in the Maritime Continent, leading to a strong IM. Another process that influences the IM is through the Indian Ocean SSTA. A basin-wide Indian Ocean warming (cooling) often occurs after a peak El Niño (La Niña) (e.g., 1983, 1988, 1995, 1998, and 1986). As seen from Fig. 10, the maximum SSTA in the tropical IO reaches to 0.6°C. The warm Indian Ocean SSTA may increase the local surface moisture and thus enhance moisture transport into India, leading a strong Indian summer monsoon (Chang and Li 2000; Li and Zhang 2002). Meanwhile, the basin-wide warming may also exert a remote impact on the WNPM through the Kelvin wave–induced anticyclonic zonal wind shear (Wu et al. 2009). This favors an out-of-phase IM–WNPM relationship.

The circulation and SST evolution patterns in 1986 are in general opposite to those shown in Fig. 10. While a strong WNPM is primarily associated with the persistence of an anomalous cyclone in WNP during the

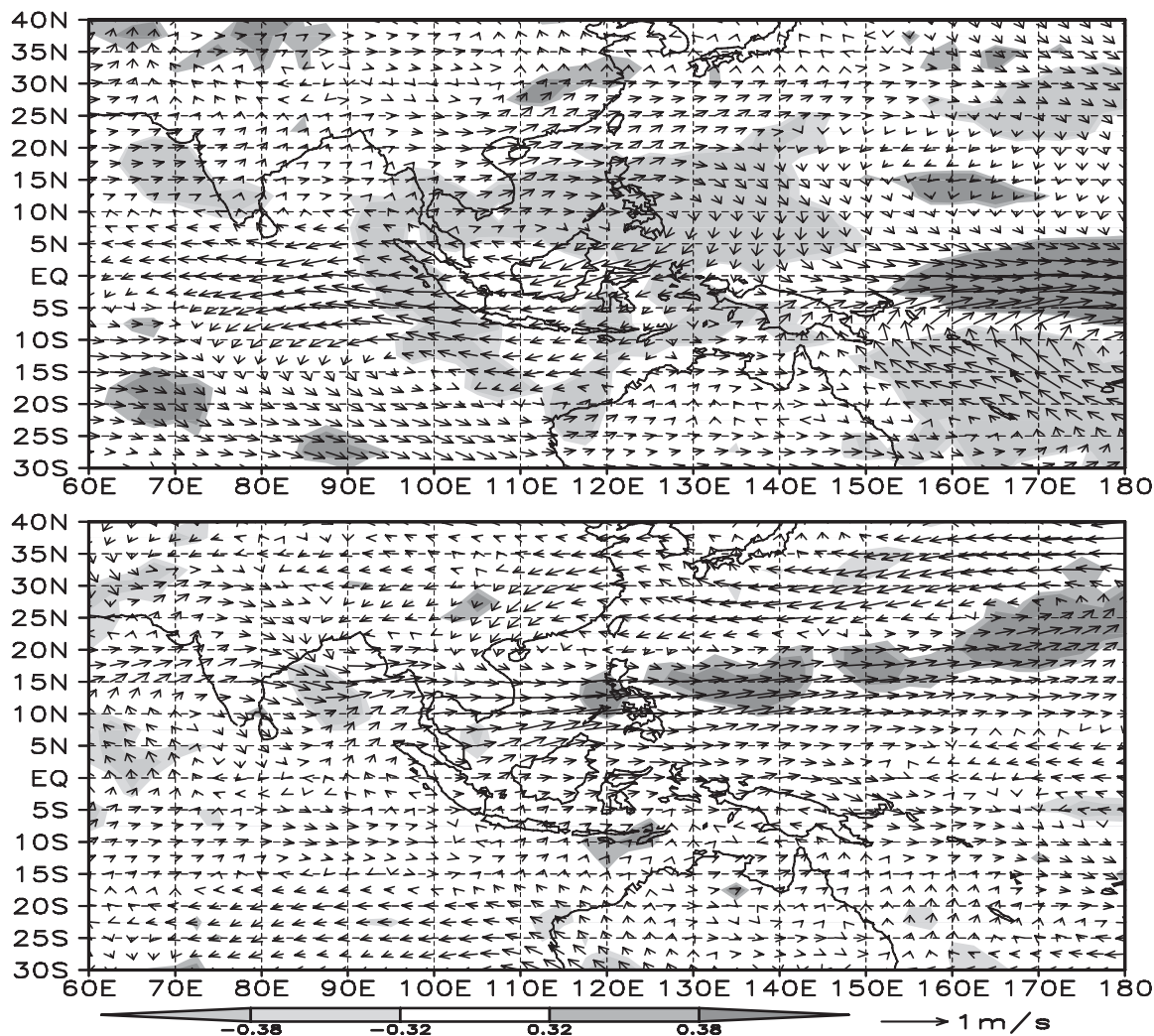


FIG. 4. As in Fig. 3, but for six-month lagged patterns association with the (top) WNP and (bottom) Australian monsoon intensity indices. The areas exceeding the 90% and 95% significant level are shaded.

La Niña decaying phase, a weak IM is attributed to both the basin-wide negative Indian Ocean SSTA (prior to the monsoon season) and the development of an El Niño in summer 1986.

## 5. Discussion

Our analysis strategy based on the submonsoon phase relationship is different from the conventional ENSO composite methodology, as the focus of this study is on the phase relations between WNPM and other submonsoon systems. As various processes may contribute to each of the monsoon in-phase and out-of-phase relationship, we further examine the circulation and SST evolution characteristics to find the common features and similar physical mechanisms that control these relationships.

Based on the observed associations aforementioned, we propose the possible schematic diagrams illustrating the essential physical processes that may contribute to each of the submonsoon phase relations. The in-phase relationship from AM to the succeeding WNPM occurs primarily during the ENSO decaying phase (Fig. 11). On the one hand, the warm SSTA in the eastern Pacific induces a reversed anomalous Walker cell and causes a weak AM during the El Niño mature winter. On the other hand, an anomalous anticyclone is induced in WNP through either the Pacific–East Asia teleconnection (Wang et al. 2000; Wang and Zhang 2002) or the eastward propagation of a low-level anticyclone anomaly in the tropical Indian Ocean (Chen et al. 2007). The WNP anomalous anticyclone is maintained through a positive local thermodynamic air–sea feedback between the anticyclone and a cold SSTA (Wang et al. 2003) from the boreal winter to

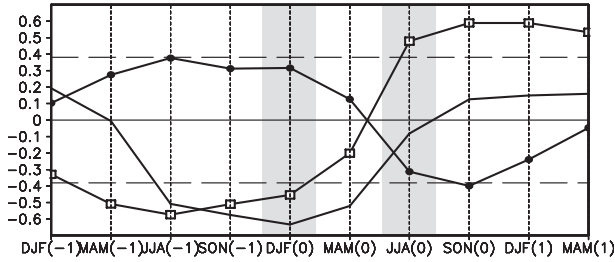


FIG. 5. Lagged correlation of the seasonal mean Niño-3.4 index with WNP (square line), Indian (dotted line), and Australian (solid line) summer monsoon intensity indices. Horizontal dashed line represents the 95% significant level and the hatched area represents monsoon active period.

late spring in the presence of the mean northeasterly. The local cold SSTA leads to a weak WNPM in boreal summer.

The out-of-phase relation from WNPM to the succeeding AM includes two different scenarios (Fig. 12).

Scenario 1 describes the El Niño early onset or the La Niña persistence events. Scenario 2 consists of El Niño decaying–La Niña developing or La Niña decaying–El Niño Modoki developing events. For the first scenario, the remote forcing of the eastern Pacific SSTA holds a key (Fig. 12a). For example, a warm SSTA forces a Rossby wave response and low-level cyclonic shear over WNP (Gill 1980), which further enhances WNPM through the Ekman pumping–induced boundary layer convergence. As the SSTA continues to develop toward the boreal winter, the same sign of the SSTA weakens the AM through the anomalous Walker circulation in boreal winter. For the second scenario, the persistence of an anomalous anticyclone during the El Niño decaying phase holds a key in inducing a weak WNPM. As the decay of an El Niño is often accompanied by the onset of La Niña in the late year, the cold SSTA in the eastern Pacific may enhance AM in boreal winter

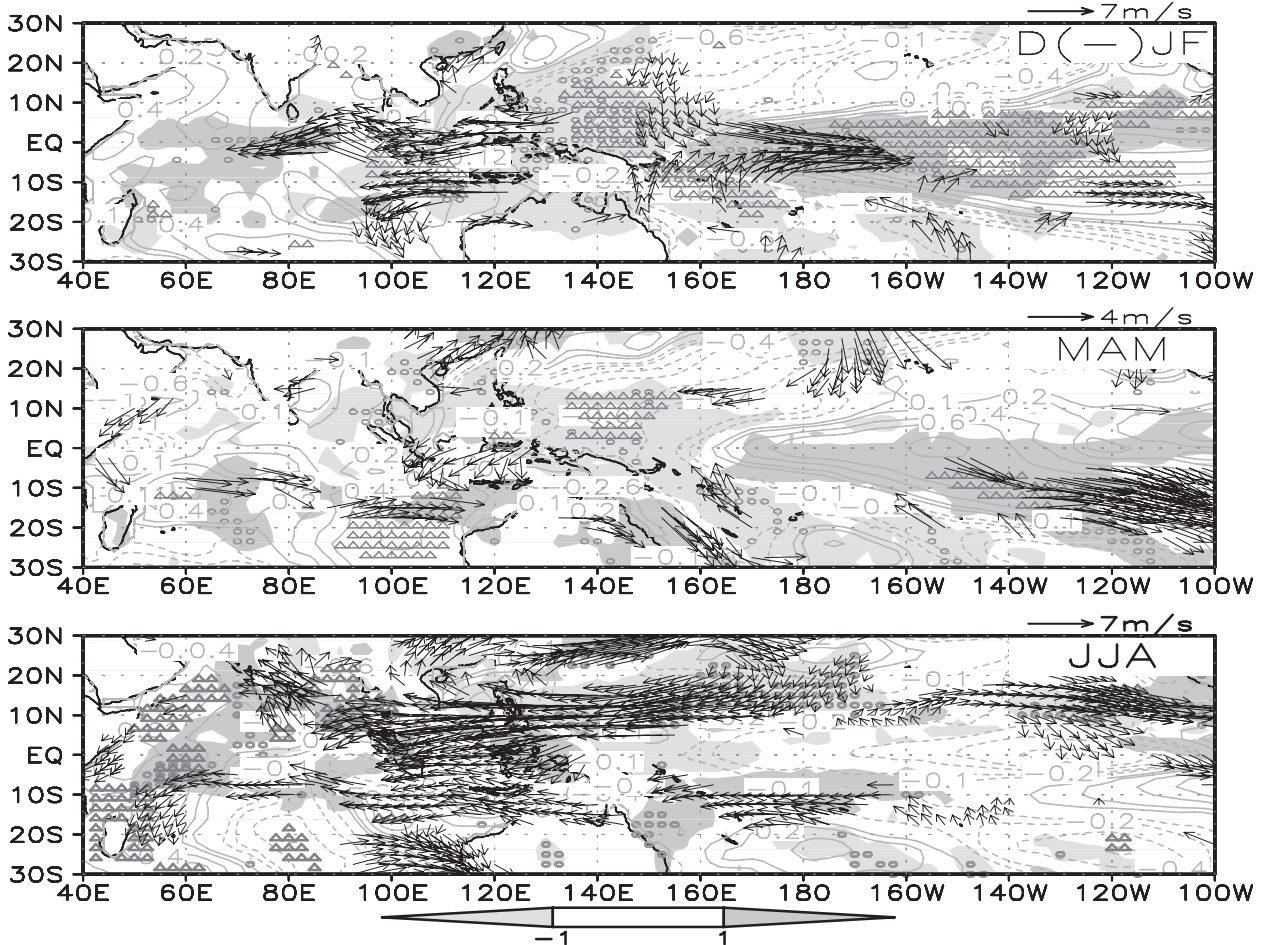


FIG. 6. The composite difference (the mean of 1983, 1988, and 1995 minus the mean of 1986 and 2001) fields of 850-hPa wind (vector,  $m s^{-1}$ , only those exceeding the 90% significant level are displayed), precipitation (shaded,  $mm day^{-1}$ , areas exceeding the 90% significant level are denoted by a circle), and SST (contour,  $^{\circ}C$ , areas exceeding the 90% significant level are denoted by a triangle) from (top to bottom) DJF to JJA. The composite is based on the normalized monsoon intensity indices that exceed 0.4 standard deviation. A Monte Carlo significance test is applied.

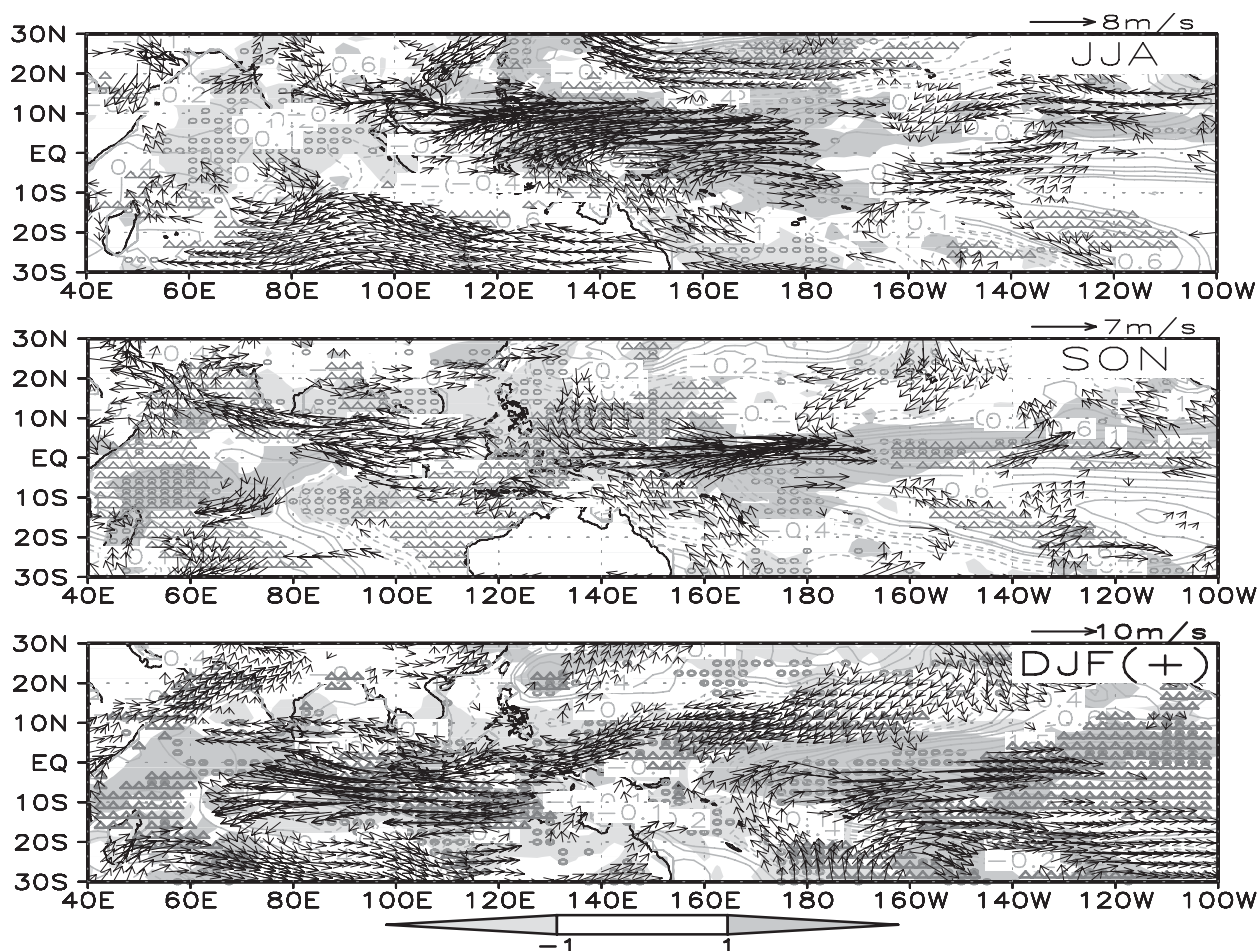


FIG. 7. As in Fig. 6, but for the mean of 1982, 1986, 2002, and 2004 minus 1996 from (top to bottom) JJA(0) to DJF(1).

through anomalous Walker circulation. Thus, the connection of WNPM and AM in the second scenario depends on both the persistence of the anomalous WNP anticyclone and the phase transition of the eastern Pacific SSTA (Fig. 12b).

The negative simultaneous correlation between WNPM and IM is mainly caused by the following two scenarios (Fig. 13). The first scenario consists of the El Niño earlier onset (or La Niña persistence) events. The SSTA in the eastern Pacific, through anomalous central equatorial heating, leads to the cyclonic wind shear in WNP and subsidence over the Maritime Continent. The former enhances the WNPM while the latter suppresses the IM (Fig. 13a). The second scenario consists of the El Niño decaying–La Niña developing (or La Niña decaying–El Niño developing) events. While a dry (wet) WNPM is attributed to the anomalous low-level anticyclone (cyclone) over WNP that persists from boreal winter to summer, a wet (dry) IM is caused by the eastern Pacific SSTA that has transitioned from a positive

(negative) to a negative (positive) episode in JJA or by a basin-wide Indian Ocean warming (cooling) that persists from El Niño (La Niña) mature winter to the subsequent summer (Fig. 13b). The basin-wide Indian Ocean warming may enhance (weaken) IM through increased (decreased) moisture transport (Chang and Li 2000; Li et al. 2001; Li and Zhang 2002).

It is worth noting that some of the strong phase relation events between simultaneous WNPM and IM and between WNPM and the subsequent AM occur at the same time. As seen from Tables 3 and 4, 1982, 1986, 2001, 2002, and 2004 are years of both simultaneous positive WNPM–negative IM phase and lagged positive WNPM–negative AM phase, and 1983, 1996, and 1998 are years of both simultaneous negative WNPM–positive IM phase and lagged negative WNPM–positive AM phase. Because of that, part of the composite evolution features looks similar in Figs. 12 and 13. It is further noted that the out-of-phase WNPM–IM relation consists of more events, such as events in 1979, 1990, 1988, and 1995.

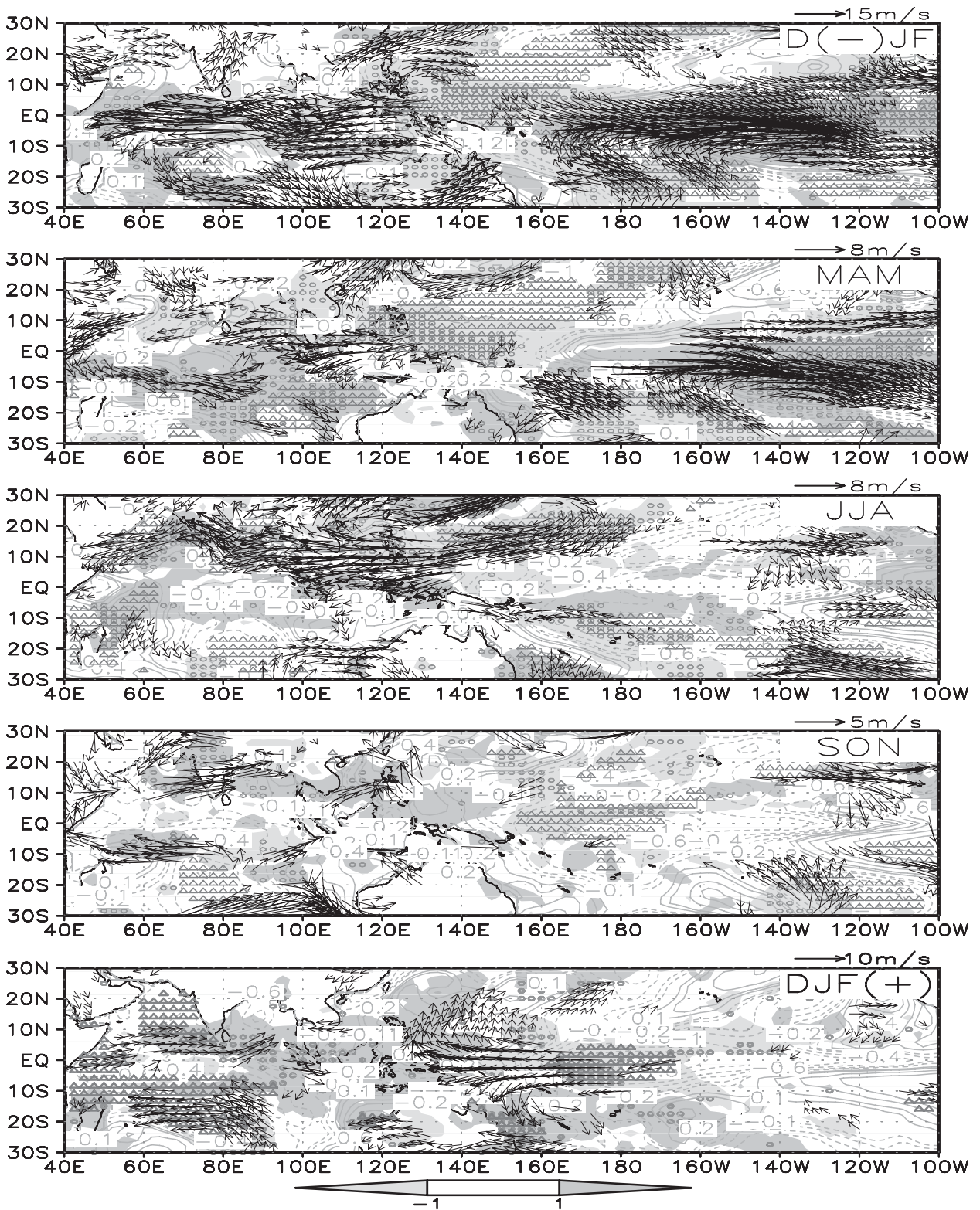


FIG. 8. As in Fig. 6, but for the mean of 1983 and 1998 minus 2001 from (top to bottom) DJF(0) to DJF(1).

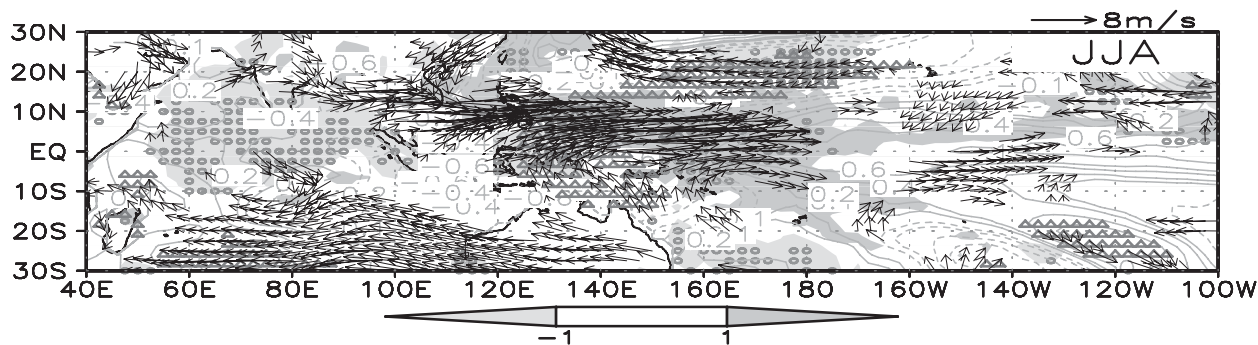


FIG. 9. As in Fig. 6, but for the mean of 1982, 1990, 2002, and 2004 minus 1996 in JJA.

Previous observational studies (e.g., Lau and Yang 1996; Li et al. 2001; Li and Zhang 2002) revealed that a warm SST anomaly in the tropical Indian Ocean leads a strong Indian monsoon. Chang and Li (2000) argued that the warm SSTA in Indian Ocean has both positive and negative effects on the Indian monsoon rainfall. A

positive SST anomaly, on the one hand, increases the local surface humidity. The increased moisture may be further transported by the mean monsoon circulation, leading to a strong monsoon. On the other hand, the positive SSTA reduces the land–sea thermal contrast and thus decreases the monsoon rainfall. Both the scale

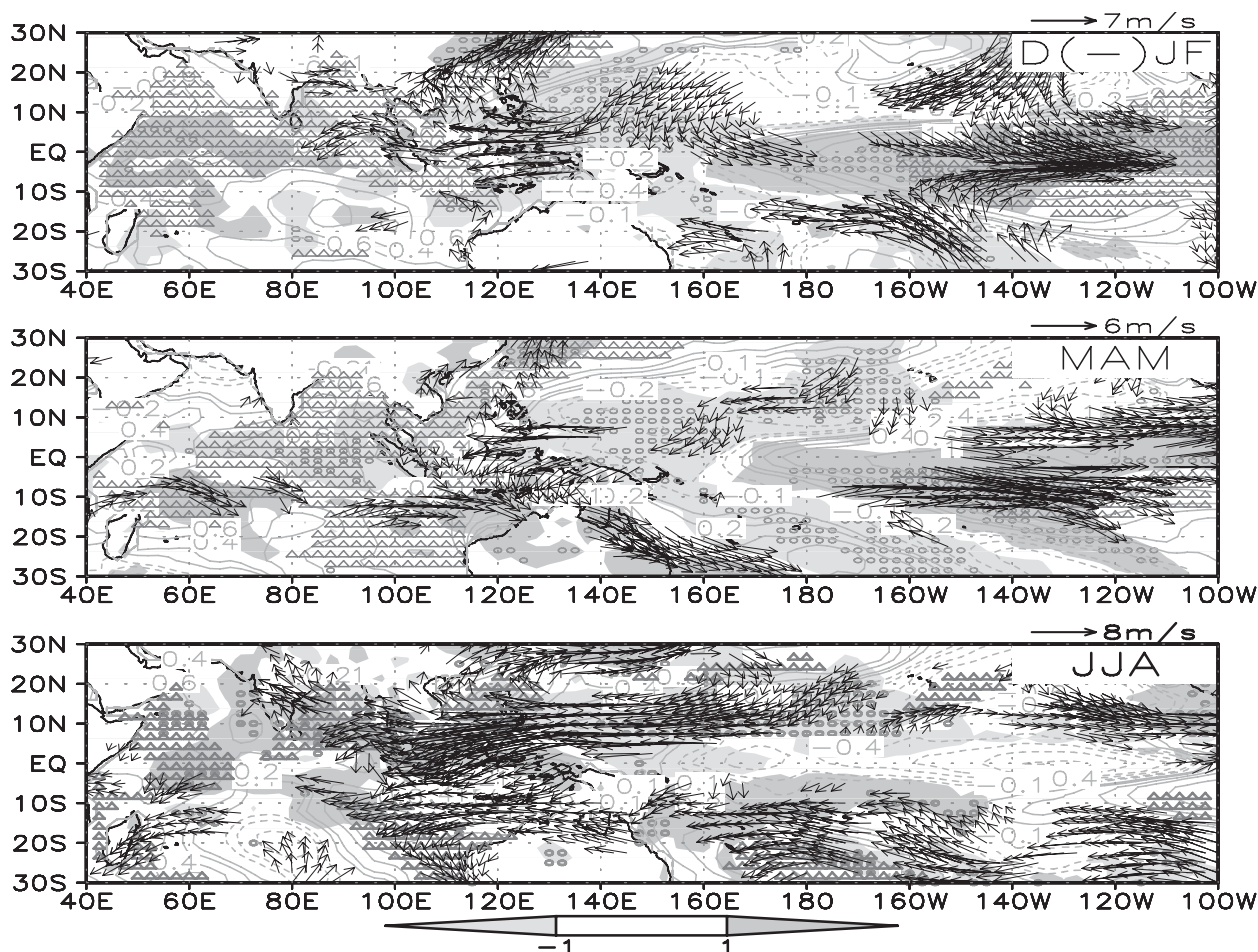


FIG. 10. As in Fig. 6, but for the mean of 1983, 1988, 1995, and 1998 minus 1986 from (top to bottom) DJF to JJA.

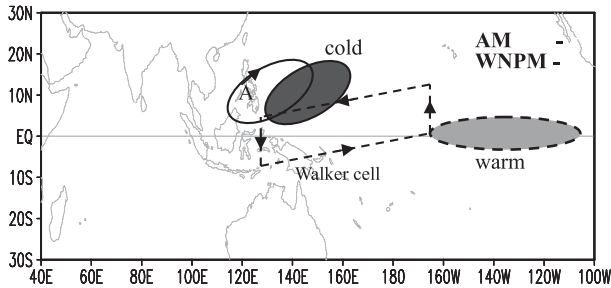


FIG. 11. Schematic diagram showing DJF (dashed line) and JJA (solid line) processes responsible for in-phase relation from AM to the succeeding WNPM.

analysis (Chang and Li 2000) and model simulations (e.g., Meehl and Arblaster 2002) showed that the positive effect is greater.

In analyzing the simultaneous IM–WNPM negative correlation, we notice a special case in summer 2001 (Fig. 14) that does not belong to both the scenarios above. As an anomalous cyclone persisted over SCS–WNP from winter to summer 2001 in association with the decay of a La Niña episode, no significant basin-wide SST anomalies appeared prior to the monsoon season in the tropical Indian Ocean, and by summer 2001 the tropical eastern Pacific SST became normal. Nevertheless, the IM was significantly weakened. The cause of the weak IM is possibly attributed to the atmospheric Rossby wave response to suppressed convection over the Maritime Continent, which, in turn, is caused by enhanced convective heating over the WNPM through the anomalous local Hadley cell (Kajikawa and Yasunari 2003). This implies that there might be a possible self-regulating process between the two submonsoon systems.

The composite analysis results above are based on the CMAP and NCEP Reanalysis-2 data. To examine the sensitivity of the aforementioned phase relationships to different data products, we conduct the same analysis procedure for two independent datasets. The first dataset includes GPCP2 rainfall and JRA reanalysis for the same period. The second dataset includes the PREC rainfall and NCEP–NCAR reanalysis for a longer period (1948–2006). Table 5 shows the lagged correlations among the three submonsoon systems using the GPCP2–JRA dataset. It is found that the correlation coefficient between WNPM and the succeeding AM is  $-0.32$ , and the correlation coefficient between WNPM and the preceding AM is  $0.32$ , both of which just pass the 90% significance level. The simultaneous correlation coefficient between WNPM and IM is  $-0.70$ , exceeding the 99% significance level. The calculation of the longer record (1948–2006) dataset of NCEP–NCAR and PREC products (see Table 6) shows that the correlation coefficient

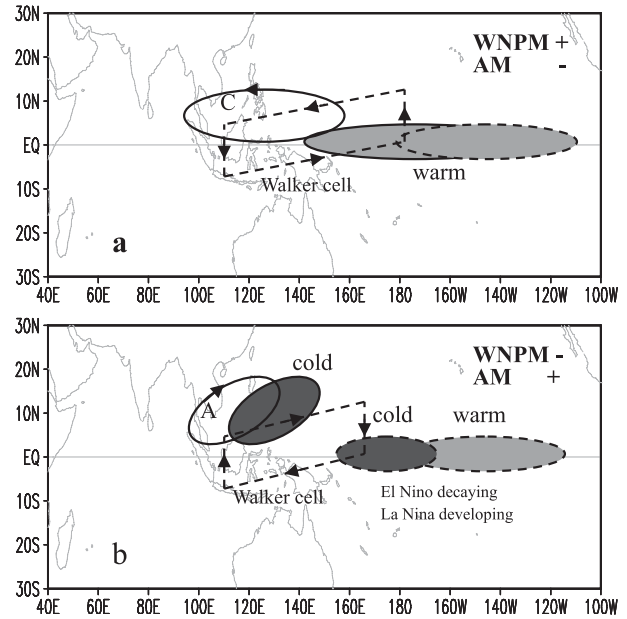


FIG. 12. Schematic diagrams showing the JJA (solid line) and DJF (dashed line) processes responsible for (a) out-of-phase relation from a strong WNPM to a weak AM and (b) out-of-phase relation from a weak WNPM to a strong AM.

between WNPM and the succeeding AM is  $-0.39$ , exceeding the 99% significance level. The simultaneous correlation coefficient between WNPM and IM is  $-0.29$ , exceeding the 95% significance level. The

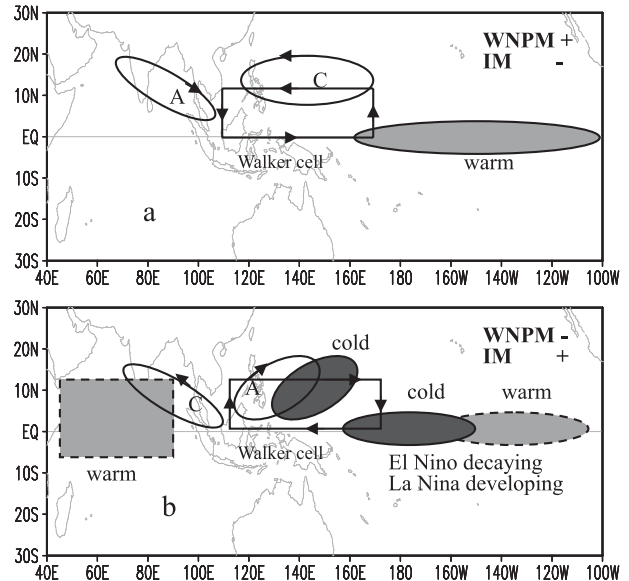


FIG. 13. Schematic diagrams showing the JJA (solid line) and DJF (dashed line) processes responsible for (a) simultaneous negative correlation between a strong WNPM and a weak IM and (b) simultaneous negative correlation between a weak WNPM and a strong IM.

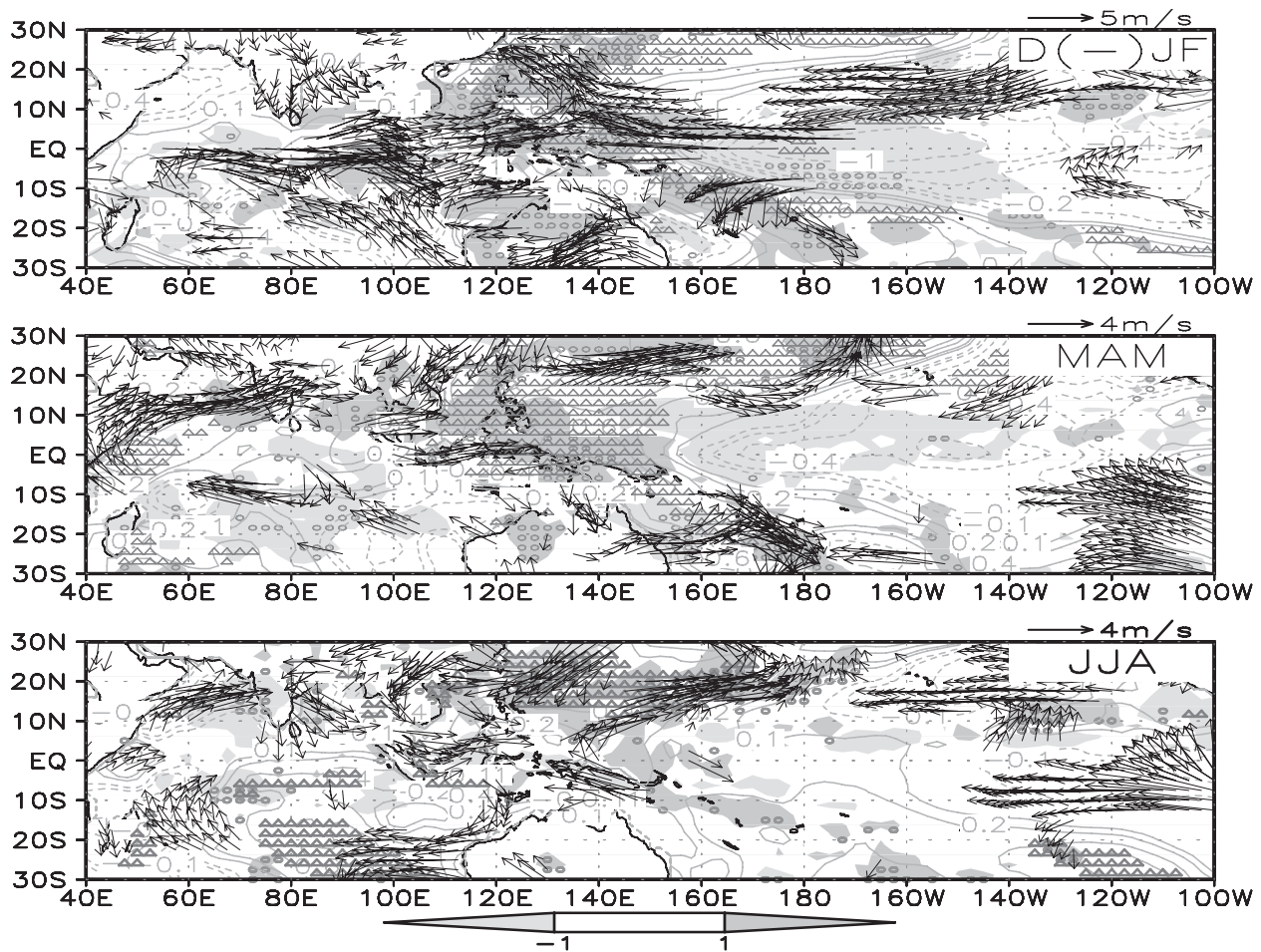


FIG. 14. Seasonal evolution patterns of 850-hPa wind (vector,  $\text{m s}^{-1}$ , only those exceeding the 90% significant level are displayed), precipitation (shaded,  $\text{mm day}^{-1}$ , areas exceeding the 90% significant level are denoted by a circle), and SST (contour,  $^{\circ}\text{C}$ , areas exceeding the 90% significant level are denoted by a triangle) from (top to bottom) DJF to JJA 2001.

lagged correlation between AM and the succeeding WNPM, however, becomes insignificant. Thus, the three datasets point out in general a robust simultaneous IM–WNPM relation and a robust lagged phase relation between WNPM and the subsequent AM, but a weak phase relation between AM and the subsequent WNPM. Thus, caution is needed when a seasonal forecast is conducted based on the weak phase relationship.

The cause of the weak correlation between AM and the subsequent WNPM is possibly attributed to the

irregular temporal evolution of La Niña events, such as the long persistent La Niña event from 1998 summer to 2001 winter. In the analysis of the NCEP–CMAP data, if we remove 1999 and 2000 data from original datasets, then the correlation coefficient between AM and the following WNPM is 0.403, exceeding the 95% significant level.

A further analysis of the longer-record data reveals that the monsoon relations are not stationary and they exhibit a marked interdecadal variability (Fig. 15). For

TABLE 5. Lagged correlation coefficients among WNPM, IM, and AM for 1979–2005 using GPCP2 and JRA data. The 90% (95%) significance level corresponds to a correlation coefficient of 0.32 (0.38). The boldface indicates a correlation exceeding the 90% significance level. The number of events indicates the number of years during which the relationship between two monsoons is consistent with the correlation coefficient.

From To	India JJA(0) Australia DJF(1)	Australia DJF(0) India JJA(0)	SCS/WNP JJA(0) Australia DJF(1)	Australia DJF(0) SCS/WNP JJA(0)	SCS/WNP JJA(0) India JJA(0)
Correlation coef	<b>0.35</b>	−0.26	<b>−0.32</b>	<b>0.32</b>	<b>−0.70</b>
No. of events	<b>17</b>	14	<b>14</b>	<b>18</b>	<b>15</b>

TABLE 6. Lagged correlation coefficients among WNPM, IM, and AM for 1948–2006 using NECP–NCAR and PREC data. The 90% (95%) significance level corresponds to a correlation coefficient of 0.22 (0.26). The boldface indicates a correlation exceeding the 90% significance level. The number of events indicates the number of years during which the relationship between two monsoons is consistent with the correlation coefficient.

From To	India JJA(0) Australia DJF(1)	Australia DJF(0) India JJA(0)	SCS/WNP JJA(0) Australia DJF(1)	Australia DJF(0) SCS/WNP JJA(0)	SCS/WNP JJA(0) India JJA(0)
Correlation coef	0.21	−0.06	−0.39	0.07	−0.29
No. of events	36	36	36	34	33

example, the significant negative correlation between WNPM and the succeeding AM appears at the beginning of 1960s, the mid-1970s, and after 1985 (Fig. 15a). The significant negative simultaneous correlation between IM and WNPM occurs after 1975 (Fig. 15b). The significant positive correlation between WNPM and the preceding AM appears from the end of 1960s to the beginning of 1970s. During other periods, the positive correlation is weak (Fig. 15c).

It is worth mentioning that the composite scenarios proposed here are based on the “after-the-fact” data (i.e., based on selected strong and weak in-phase or out-of-phase events). While such an analysis strategy helps us to understand multiple processes that contribute to the in-phase and out-of-phase relations, it may have a limited application in real forecast. The mechanisms discussed here are primarily based on the boundary SSTA forcing. As we know, in addition to the lower boundary forcing, the monsoons are also influenced by internal atmospheric variabilities including synoptic and intraseasonal oscillations. Some cases, for example, 1979 and 1981 in Table 2, cannot be simply explained by the lower boundary forcing. It is desirable to further study these cases in future work.

## 6. Conclusions

In this study we investigate the phase relationships of the SCS–WNP summer monsoon (WNPM) with the Australian monsoon (AM) and Indian monsoon (IM). Based on the analysis of the mean and standard deviation of the CMAP precipitation and relative vorticity fields, we define the monsoon intensity indices for the Australian, WNP, and Indian summer monsoons. The indices well represent the large-scale rainfall and low-level circulation patterns over each of the three sub-monsoon regions.

It is found that WNPM has significant lead–lag phase relationships with AM and IM. The correlation coefficient between WNPM and the succeeding AM is  $-0.41$ , passing the 95% significance level. The correlation coefficient between WNPM and the preceding AM is  $0.37$ , and is also significant but only passes the 90% significance level. The maximum correlation appears simultaneous between

WNPM and IM. The correlation coefficient is  $-0.64$ , exceeding the 99% significance level. Using the two other datasets is generally consistent with the conclusion above.

By examining the circulation and SST patterns and evolution characteristics, several possible mechanisms are proposed to explain the observed in-phase and out-of-phase relationships. While the Australian summer monsoon is mainly controlled by simultaneous SSTA in the equatorial eastern Pacific, the Indian and WNP summer monsoons may be determined by various factors including the local SSTA in the tropical Indian Ocean and

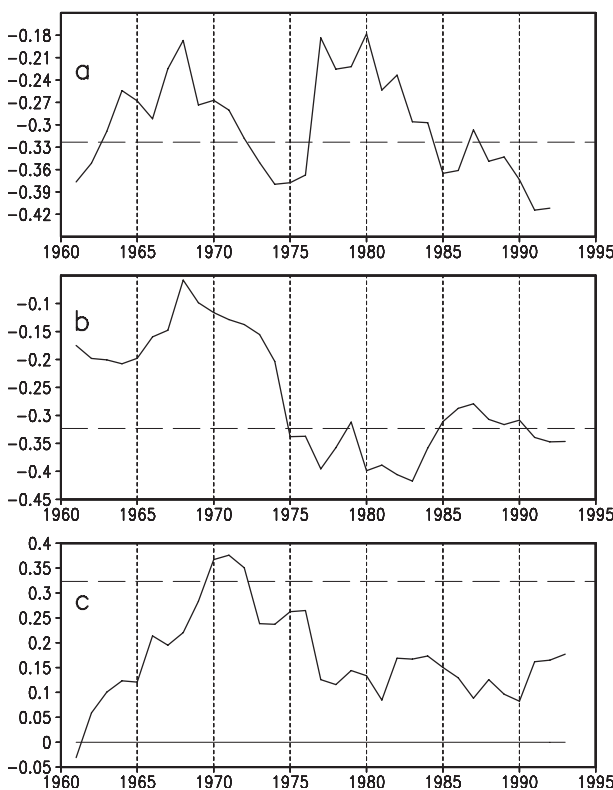


FIG. 15. The 27-yr window moving correlation coefficient between (a) WNPM and the succeeding AM; (b) IM and WNPM; and (c) WNPM and the preceding AM based on NCEP–NCAR reanalysis and PREC data for 1948–2006. Horizontal dashed lines represent the 90% significance level and horizontal solid lines represent zero.

western Pacific and anomalous convection over the Maritime Continent.

The in-phase relationship from AM to the succeeding WNPM occurs primarily during the ENSO decaying phase. A warm SSTA in the eastern Pacific weakens AM through anomalous Walker circulation during the El Niño mature winter. The persistence of an anomalous anticyclone in WNP due to local air–sea interactions (Wang et al. 2000) further leads to a weak WNPM.

The out-of-phase relation from WNPM to the succeeding AM involves two possible processes. For the first scenario, an El Niño develops so early that the warm SSTA in the eastern Pacific in JJA is able to force a low-level cyclonic flow anomaly over WNP, which further enhances WNPM. As the SSTA matures toward boreal winter, it weakens the AM through the anomalous Walker circulation. The second scenario happens during the El Niño decaying phase. On the one hand, the persistence of the WNP anomalous anticyclone causes a weak WNPM. On the other hand, the phase transition of a warm to a cold episode leads to a strong AM in DJF.

The simultaneous negative correlation between WNPM and IM often appears either during the El Niño early onset years or during the El Niño decaying (La Niña developing) summer. In the former, a warm SSTA in the eastern Pacific on one hand induces the cyclonic wind shear and strengthens WNPM, and on the other hand causes anomalous subsidence over the Maritime Continent, which further suppresses convection over India through the atmospheric Rossby wave response (Wang et al. 2003). In the latter, a weak WNPM results from the persistence of the WNP anomalous anticyclone, whereas a strong IM is caused by a cold eastern Pacific SSTA (due to the El Niño phase transition), a basin-wide Indian Ocean warming [through the remote Kelvin wave-forcing effect, see Wu et al. (2009) and Xie et al. (2009)], or enhanced convection in the Maritime Continent associated with the local Hadley circulation in the WNP.

*Acknowledgments.* The authors thank Dr. Black, Dr. J. Fasullo, and two anonymous reviewers for constructive comments, which greatly improve the original manuscript. This work was supported by the National Science Foundation of China under Contracts 40675054 and 40505019 and by China Meteorological Administration under Contract CMATG2006L03. TL was also supported by ONR Grant N000140810256 and by the International Pacific Research Center that is sponsored by the Japan Agency for Marine-Earth Science and Technology (JAMSTEC), NASA (NNX07AG53G), and NOAA (NA17RJ1230). This work is also supported by the Knowledge Innovation Project of the Chinese Academy of Sciences (KZCX2-YW-BR-04). The authors acknowledge

NOAA for providing NCEP–DOE, CMAP, GPCP, NCEP–NCAR reanalysis and PREC data, and JMA and CRIEPI for providing JRA-25 reanalysis data (downloads available at <http://www.cdc.noaa.gov/> and <http://jra.kishou.go.jp/>).

## REFERENCES

- Adler, R. F., and Coauthors, 2003: The version 2 Global Precipitation Climatology Project (GPCP) monthly precipitation analysis (1979–present). *J. Hydrometeorol.*, **4**, 1147–1167.
- Ashok, K., S. K. Behera, S. A. Rao, H. Weng, and T. Yamagata, 2007: El Niño Modoki and its possible teleconnection. *J. Geophys. Res.*, **112**, C11007, doi:10.1029/2006JC003798.
- Chang, C.-P., and T. Li, 2000: A theory for the tropical tropospheric biennial oscillation. *J. Atmos. Sci.*, **57**, 2209–2224.
- , P. A. Harr, and J. Ju, 2001: Possible roles of Atlantic circulations on the weakening Indian monsoon rainfall–ENSO relationship. *J. Climate*, **14**, 2376–2380.
- Chen, J.-M., T. Li, and C.-F. Shih, 2007: Fall persistence barrier of sea surface temperature in the South China Sea associated with ENSO. *J. Climate*, **20**, 158–172.
- Chen, M., P. Xie, J. E. Janowiak, and P. A. Arkin, 2004: Verifying the reanalysis and climate models outputs using a 56-year data set of reconstructed global precipitation. Preprints, *14th Conf. on Applied Meteorology*, Seattle, WA, Amer. Meteor. Soc., J6.1 [Available online at <http://ams.confex.com/ams/pdfpapers/70083.pdf>].
- Fasullo, J., 2004: Biennial characteristics of all India rainfall. *J. Climate*, **17**, 2972–2982.
- Gill, A. E., 1980: Some simple solutions for heat-induced tropical circulation. *Quart. J. Roy. Meteor. Soc.*, **106**, 447–462.
- Gregory, S., 1991: Interrelationship between Indian and northern Australia summer monsoon rainfall values. *Int. J. Climatol.*, **11**, 55–62.
- Hung, C. W., X. D. Liu, and M. Yanai, 2004: Symmetry and asymmetry of the Asian and Australian summer monsoons. *J. Climate*, **17**, 2413–2426.
- Kajikawa, Y., and T. Yasunari, 2003: The role of the local Hadley circulation over the western Pacific on the zonally asymmetric anomalies over the Indian Ocean. *J. Meteor. Soc. Japan*, **81**, 259–276.
- Kalnay, E., and Coauthors, 1996: The NCEP/NCAR 40-Year Reanalysis Project. *Bull. Amer. Meteor. Soc.*, **77**, 437–471.
- Kanamitsu, M., W. Ebisuzaki, J. Woollen, S.-K. Yang, J. J. Hnilo, M. Fiorino, and G. L. Potter, 2002: NCEP–DEO AMIP-II Reanalysis (R-2). *Bull. Amer. Meteor. Soc.*, **83**, 1631–1643.
- Krishnamurthy, V., and B. N. Goswami, 2000: Indian monsoon–ENSO relationship on interdecadal timescale. *J. Climate*, **13**, 579–595.
- Kumar, K. K., B. Rajagopalan, and M. C. Cane, 1999: On the weakening relationship between the Indian monsoon and ENSO. *Science*, **284**, 2156–2159.
- Lau, K.-M., and S. Yang, 1996: The Asian monsoon and the predictability of the tropical ocean–atmosphere system. *Quart. J. Roy. Meteor. Soc.*, **122**, 945–957.
- Li, T., and Y. Zhang, 2002: Processes that determine the quasi-biennial and lower-frequency variability of the South Asian monsoon. *J. Meteor. Soc. Japan*, **80**, 1149–1163.
- , —, C. P. Chang, and B. Wang, 2001: On the relationship between Indian Ocean SST and Asian summer monsoon. *Geophys. Res. Lett.*, **28**, 2843–2846.

- , P. Liu, X. Fu, B. Wang, and G. A. Meehl, 2006: Spatiotemporal structures and mechanisms of the tropospheric biennial oscillation in the Indo-Pacific warm ocean regions. *J. Climate*, **19**, 3070–3087.
- Livezey, R. E., and W. Y. Chen, 1983: Statistical field significance and its determination by Monte Carlo techniques. *Mon. Wea. Rev.*, **111**, 46–59.
- Matsumoto, J., 1992: The seasonal changes in Asian and Australian regions. *J. Meteor. Soc. Japan*, **70**, 257–273.
- Meehl, G. A., 1987: The annual cycle and interannual variability in the tropical Indian and Pacific Ocean regions. *Mon. Wea. Rev.*, **115**, 27–50.
- , and J. M. Arblaster, 2002: GCM sensitivity experiments for the Indian monsoon and tropospheric biennial oscillation transition conditions. *J. Climate*, **15**, 923–944.
- Onogi, K., and Coauthors, 2007: The JRA-25 reanalysis. *J. Meteor. Soc. Japan*, **85**, 369–432.
- Smith, T. M., and R. W. Reynolds, 2004: Improved extended reconstruction of SST (1854–1997). *J. Climate*, **17**, 2466–2477.
- Wang, B., and Q. Zhang, 2002: Pacific–East Asian teleconnection. Part II: How the Philippine Sea anticyclone established during development of El Niño. *J. Climate*, **15**, 3252–3265.
- , R. Wu, and X. Fu, 2000: Pacific–East Asia teleconnection: How does ENSO affect East Asian climate? *J. Climate*, **13**, 1517–1536.
- , —, and T. Li, 2003: Atmosphere–warm ocean interaction and its impact on Asian–Australian monsoon variation. *J. Climate*, **16**, 1195–1211.
- Wolter, K., R. M. Dole, and C. A. Smith, 1999: Short-term climate extremes over the continental United States and ENSO. Part I: Seasonal temperatures. *J. Climate*, **12**, 3255–3272.
- Wu, B., T. Zhou, and T. Li, 2009: Seasonally evolving dominant interannual variability modes of East Asian climate. *J. Climate*, **22**, 2992–3005.
- , —, and —, 2010: Relative contributions of the Indian Ocean and local SST anomalies to the maintenance of the western North Pacific anomalous anticyclone during the El Niño decaying summer. *J. Climate*, **23**, 2974–2986.
- Wu, R., and B. P. Kirtman, 2007a: Role of Indian Ocean in the biennial transition of the Indian summer monsoon. *J. Climate*, **20**, 2147–2164.
- , and —, 2007b: Roles of the Indian Ocean in the Australian summer monsoon–ENSO relationship. *J. Climate*, **20**, 4768–4787.
- Xie, P., and P. A. Arkin, 1997: Global precipitation: A 17-year monthly analysis based on gauge observations, satellite estimates, and numerical model outputs. *Bull. Amer. Meteor. Soc.*, **78**, 2539–2558.
- Xie, S.-P., K. Hu, J. Hafner, H. Tokinaga, Y. Du, G. Huang, and T. Sampe, 2009: Indian Ocean capacitor effect on Indo-western Pacific climate during the summer following El Niño. *J. Climate*, **22**, 730–747.
- Zhang, Y., and T. Li, 2008: Influence of the tropical sea surface temperature in the Indian–Pacific Ocean on the relationship between the South Asian and North Australian summer monsoons. *Terr. Atmos. Oceanic Sci.*, **19**, 321–329.